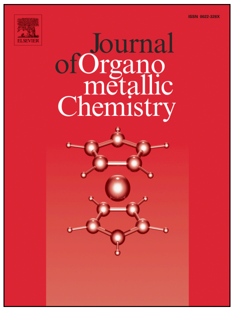

Long-distance electronic coupling in diferrocenyl compounds with cross-conjugated *germinal*-diethynylethene bridges

Yang Fan, Hua-Min Li, Guo-Dong Zou, Xu Zhang, Meng Li, Jia-Hui Wu, Xin Zhang, Hai-Ting Lu

PII: S0022-328X(18)30070-6

DOI: 10.1016/j.jorganchem.2018.01.052

Reference: JOM 20290

To appear in: *Journal of Organometallic Chemistry*

Received Date: 28 October 2017

Revised Date: 17 January 2018

Accepted Date: 29 January 2018

Please cite this article as: Y. Fan, H.-M. Li, G.-D. Zou, X. Zhang, M. Li, J.-H. Wu, X. Zhang, H.-T. Lu, Long-distance electronic coupling in diferrocenyl compounds with cross-conjugated *germinal*-diethynylethene bridges, *Journal of Organometallic Chemistry* (2018), doi: 10.1016/j.jorganchem.2018.01.052.

Long-distance electronic coupling in diferrocenyl compounds with cross-conjugated *germinal*-diethynylethene bridges

Yang Fan[a, *], Hua-Min Li[a], Guo-Dong Zou[a], Xu Zhang[b], Meng Li[a], Jia-Hui Wu[a], Xin Zhang, Hai-Ting Lu[a]

[a]College of Chemistry and Chemical Engineering, Xinyang Normal University, Xinyang 464000, China

[b]Fujian Institute of Research on the Structure of Matter, Chinese Academy of Sciences, Fuzhou 350002, China

Abstract: A series of *germinal*-diethynylethene (*gem*-DEE) bridged diferrocenyl compounds, including 1,1-[bis(ferrocenylethynyl)methylene]cyclohexane (**1**), 1,1-[bis(ferrocenylethynyl)methylene]tetrahydro-2*H*-pyran (**2**), and 1,1-[bis(ferrocenylethynyl)methylene]tetrahydro-2*H*-thiopyran (**3**) were synthesized and characterized. The Fe···Fe distance between the two ferrocenyl termini reaches up to ~9 Å for compounds **2** and **3**. The electrochemical measurements demonstrate moderate electronic coupling between the *gem*-DEE-bridged ferrocenyl (Fc) termini in this cross-conjugated system. UV-vis-NIR spectroscopy studies suggest that the monocation species of these compounds belong to class II mixed-valence systems in Robin–Day classification. DFT calculations further reveal electronic structures of these cross-conjugated diferrocenyl compounds.

Keywords: Diferrocenyl; Diethynylethene; Cross-conjugated; Electronic coupling; Mixed-valence.

1. Introduction

The binuclear and poly-nuclear mixed-valence metal complexes with π conjugated bridging ligand have attracted continuous interests for decades, which offer a good deal of molecular models for the fundamental study of electron transfer processes [1–26]. In particular, the long-distance electronic coupling involving metal–metal distance up to nanometer-scale is of great importance from both fundamental and practical point of view [27–30]. These nanometer-scale molecular systems with controllable electron transfer properties have potential applications in molecular electronics and optoelectronic materials. For instance, Ren and co-workers reported a series of $Ru_2(Xap)_4$ (ap = 2-anilinopyridinate) capped polyyn-diyl (μ-C_{2m}, m = 4–10) diruthenium compounds with the distance between two Ru_2 termini up to ~28 Å [28]. It is revealed that the electronic coupling between the Ru_2 termini depends on the length of polyyn-diyl with an attenuation constant between 0.12 and 0.15 $Å^{-1}$. These results provide in-depth understanding on the long-distance electron transfer mediated by polyyn-diyl bridge.

Compared to the extensively investigated linearly conjugated bridging ligands, the redox-active binuclear complexes bridged by cross-conjugated ligands have only been started to be explored in recent years [31–40]. The weak electronic coupling between two Fc centers bridged by the cross-conjugated 3-(dibromomethylidene)penta-1,4-diyne ligand was firstly reported by Xu *et al* [35]. The Fe···Fe distance in the crystal structure of this diferrocenyl compound reaches to ~10.5 Å. The diruthenium compounds bearing cross-conjugated *σ-geminal*-diethynylethene (*gem*-DEE) ligand exhibit attenuated electronic coupling between the two Ru_2 termini compared to that of the counterpart with buta-1,3-diyne bridge [36]. In the recent report by Low and co-workers, using the weakly coordinating electrolyte n-Bu$_4$N[B{C$_6$H$_3$(CF$_3$)$_2$-3,5}$_4$], the electronic coupling was more clearly resolved in cross-conjugated bis- and tris-ferrocenyl complexes Ph$_2$C=C(C≡CFc)$_2$ and FcCH=C(C≡CFc)$_2$ with Fe···Fe distance up to ~10.3 Å [33]. The weakly coordinating electrolyte Na[B{C$_6$H$_3$(3,5-CF$_3$)$_2$}$_4$] was also used in our recent investigation on the electron transfer properties of a series of *gem*-DEE bridged diferrocenyl compounds [40].

Herein we reported the syntheses, voltammetric and spectroscopic studies of a series of diferrocenyl compounds bridged by cross-conjugated *gem*-DEE ligands with different pendent substituents including cyclohexane, tetrahydro-2*H*-pyran, and tetrahydro-2*H*-thiopyran. The single-crystal X-ray diffraction analyses reveal that the Fe···Fe distances between the Fc termini in the crystal structures of these compounds reaches up to ~9 Å for compounds **2** and **3**. The experimental and computational studies suggest that these cross-conjugated diferrocenyl compounds belong to the weakly coupled Robin–Day class II systems.

2. Experimental

2.1. Reagents

Tetrabromomethane (98%), cyclohexanone (99%), tetrahydro-4*H*-pyran-4-one (98%), tetrahydro-4*H*-thiopyran-4-one (98%), triphenylphosphine (99%), heptane (98%), triethylamine (99%) and NOBF$_4$ (98%) was purchased from commercial suppliers. These reagents were used as received without further purification. Ethynylferrocene [41], (1,1-dibromomethylene)cyclohexane [42], and Na[B{C$_6$H$_3$(3,5-CF$_3$)$_2$}$_4$] [43] were synthesized by literature methods.

2.2. Instruments

^{1}H and ^{13}C NMR spectra were recorded on a Bruker BioSpin GmbH 600 MHz spectrometer using $CDCl_3$ as solvent. Chemical shifts were reported in ppm relative to internal TMS (0 ppm). Elemental analyses were performed using a Vario MICRO elemental analyzer. UV–vis–NIR spectra of the samples in CH_2Cl_2 solutions were obtained on PerkinElmer Lamda-950 spectrophotometer.

2.3. Single-crystal X-ray diffraction analysis

The X-ray diffraction data for compounds **1–3** were collected on a Xcalibur Eos Gemini CCD diffractometer with graphite–monochromated Mo Kα radiation (λ = 0.71073 Å) at room temperature. The structures were solved by direct methods and refined by full-matrix least-squares on F^2 by using the program SHELX-2016 [44]. Anisotropic thermal factors were assigned to all the non-hydrogen atoms. The positions of the hydrogen atoms were generated geometrically, assigned isotropic thermal parameters, and allowed to ride on their respective parent atoms before the final cycle of least-squares refinement. Detailed crystal data and structure refinements parameters for compounds **1–3** are listed in Table S1. Further crystallographic details for the compounds are summarized in CCDCs 1582342 (**1**), 1582343 (**2**) and 1582344 (**3**).

2.4. Electrochemistry

The electrochemical experiments were carried out with a CHI 660E electrochemical workstation (CH Instruments). Cyclic voltammetry (CV) and differential pulse voltammetry

(DPV) measurements were performed using a three-electrode system with a glassy carbon working electrode, a Pt wire counter electrode, and a Ag/AgCl (3 M KCl) reference electrode in CH_2Cl_2 solution containing 0.01 M $Na[B\{C_6H_3(3,5\text{-}CF_3)_2\}_4]$ (N_2-degassed) as electrolyte.

2.5. DFT calculations

DFT calculations were carried out using *Gaussian 09* software with the B3LYP exchange-correlation functional and 6-31G** basis set. Geometry optimizations of the structures were done using parameters from the corresponding crystal structure data as starting points. No symmetry constraints were used in the optimization. The optimized geometries were fully characterized as true minima via analytical frequency calculations (no imaginary eigenvalues). The solvent (CH_2Cl_2) effects were considered using the polarized continuum model (PCM).

2.6. Syntheses of compounds ***1–3***

*2.6.1. Synthesis of 1,1-[bis(ferrocenylethynyl)methylene]cyclohexane (**1**)*

A mixture of (1,1-dibromomethylene)cyclohexane (100 mg, 0.4 mmol), ethynylferrocene (189 mg, 0.9 mmol), $Pd(PPh_3)_2Cl_2$ (30 mg, 0.04 mmol) and CuI (20 mg, 0.1 mmol) in triethylamine (5 mL) was sealed in a 120 mL Teflon screwed tube under N_2 atmosphere. The reaction mixture was heated at 95 ^{o}C with stirring for 24 h. After cooling to room temperature, the reaction mixture was diluted with CH_2Cl_2 (100 mL), washed with saturated aq. NH_4Cl solution (2 × 50 mL) and distilled water (2 × 50 mL). The organic layer was dried over anhydrous Na_2SO_4, and concentrated under reduced pressure. The crude product was purified by column chromatography on silica gel (CH_2Cl_2 : petroleum ether = 1 : 5) to yield the title compound **1** as red solid (105 mg, 51% yield). ^1H NMR (600 MHz, $CDCl_3$): δ 4.47 (s, 4H, C_5H_4), 4.23 (s, 10H, C_5H_5), 4.19 (s, 4H, C_5H_4), 2.57 (s, 4H, CH_2), 1.66 (s, 4H, CH_2), 1.62 (s, 2H, CH_2). ^{13}C NMR (150 MHz, $CDCl_3$): δ 158.82, 98.75, 89.51, 82.65, 71.38, 69.93, 68.68, 65.67, 32.86, 27.56, 26.28. Anal. Calcd for $C_{31}H_{28}Fe_2$: C, 72.69; H, 5.51. Found: C, 72.90; H, 5.54.

2.6.2. *Synthesis of 4-(dibromomethylene)tetrahydro-2H-pyran (**2a**)*

In an oven-dried three-necked flask, a mixture of tetrahydro-4*H*-pyran-4-one (1.0 g, 10 mmol), CBr_4 (6.63 g, 20 mmol), PPh_3 (10.5 g, 40 mmol) in heptane (100 mL) was refluxed under N_2 atmosphere for 48 h. After cooling to room temperature, the reaction mixture was filtered through Celite, and the solid residue was washed with petroleum ether. The solvent was removed under reduced pressure to give crude products. Chromatography on silica gel using petroleum ether as the eluent afforded the product as white solid (1.3 g, 51% yield). ^1H NMR (600 MHz, $CDCl_3$): δ 3.68 (t, J = 4.9 Hz, 4H, CH_2), 2.51 (t, J = 4.9 Hz, 4H, CH_2). ^{13}CNMR (150 MHz, $CDCl_3$): δ 139.96, 84.49, 67.37, 35.15. Anal. Calcd for $C_6H_8OBr_2$: C, 28.16; H, 3.15. Found: C, 28.31; H, 3.16.

*2.6.3. Synthesis of 1,1-[bis(ferrocenylethynyl)methylene]tetrahydro-2H-pyran (**2**)*

This compound was prepared from **2a** by the same procedure for that of **1**. Chromatography on silica gel (CH_2Cl_2 : petroleum ether = 1 : 1) gave the desired product as red solid (120 mg, 59% yield). ^1H NMR (600 MHz, $CDCl_3$): δ 4.47 (s, 4H, C_5H_4), 4.23 (s, 10H, C_5H_5), 4.21 (s, 4H, C_5H_4), 3.78 (t, J = 4.4 Hz, 4H, CH_2), 2.69 (t, J = 4.3 Hz, 4H, CH_2). ^{13}C NMR (150 MHz, $CDCl_3$): δ 151.75, 100.65, 90.70, 81.90, 71.41, 69.97, 68.86, 68.18, 65.17, 33.28. Anal. Calcd for $C_{30}H_{26}OFe_2$: C, 70.07; H, 5.10. Found: C, 70.15; H, 5.11.

*2.6.4. Synthesis of 4-(dibromomethylene)tetrahydro-2H-thiopyran (**3a**)*

This compound was prepared from tetrahydro-4*H*-thiopyran-4-one by the same procedure for that of **2a**. Chromatography on silica gel using petroleum ether as eluent gave the desired product as light yellow solid (1.5 g, 56% yield). ^{1}H NMR (600 MHz, $CDCl_3$): δ 2.76 (d, J = 5.3 Hz, 4H, CH_2), 2.70 (d, J = 5.4 Hz, 4H, CH_2). ^{13}C NMR (150 MHz, $CDCl_3$): δ 141.99, 85.43, 36.62, 29.27. Anal. Calcd for $C_6H_8SBr_2$: C, 26.49; H, 2.96. Found: C, 26.61; H, 2.98.

*2.6.5. Synthesis of 1,1-[bis(ferrocenylethynyl)methylene]tetrahydro-2H-thiopyran (**3**)*

This compound was prepared from **3a** by the same procedure for that of **1**. Chromatography on silica gel (CH_2Cl_2 : petroleum ether = 1 : 1) gave the desired product as red solid (115 mg, 54% yield). ^{1}H NMR (600 MHz, $CDCl_3$): δ 4.47 (s, 4H, C_5H_4), 4.24 (s, 10H, C_5H_5), 4.22 (s, 4H, C_5H_4), 2.92 (s, 4H, CH_2), 2.78 (d, J = 4.2 Hz, 4H, CH_2). ^{13}C NMR (150 MHz, $CDCl_3$): δ 153.77, 101.56, 91.18, 81.92, 71.42, 69.96, 68.89, 65.08, 34.38, 30.16. Anal. Calcd for $C_{30}H_{26}SFe_2$: C, 67.95; H, 4.94. Found: C, 68.09; H, 4.95.

3. Results and discussion

The *gem*-DEE bridged diferrocenyl compounds (Fig. 1) were readily synthesized from the ketones, including cyclohexanone, tetrahydro-4*H*-pyran-4-one and tetrahydro-4*H*-thiopyran-4-one, by the Corey-Fuchs olefination and subsequent Sonogashira coupling with ethynylferrocene (Scheme 1). The resulting compounds 1,1-[bis(ferrocenylethynyl)methylene]cyclohexane (**1**), 1,1-[bis(ferrocenylethynyl)methylene]tetrahydro-2*H*-pyran (**2**), and 1,1-[bis(ferrocenylethynyl)methylene]tetrahydro-2*H*-thiopyran (**3**), and the 1,1-dibromoalkene intermediates 4-(dibromomethylene)tetrahydro-2*H*-pyran (**2a**) and 4-(dibromomethylene)tetrahydro-2*H*-thiopyran (**3a**) were characterized by NMR spectroscopy and elemental analysis. The diferrocenyl compounds are all stable under ambient conditions in solution or in the solid state.

The molecular structures of compounds **1**–**3** were determined by single-crystal X-ray diffraction analysis (Fig. 2). The compounds crystalize in the triclinic space group P-1 (**1**) and the monoclinic space group $P2_1/c$ (**2** and **3**) with one crystallographically independent molecule in the asymmetric unit (Table S1). As shown in Fig. 2, the central *gem*-DEE backbone exhibits a typical planar Y-shape geometry. The C≡C and C=C bond lengths in the *gem*-DEE backbone as well as the alkylidene bond angles are comparable to other cross-conjugated enediynes (Table 1). A typical chair conformation was observed for the cyclohexane and tetrahydro-2*H*-thiopyran pendent substituents in compounds **1** and **3**, respectively, while the tetrahydro-2*H*-pyran substituent in **2** exhibits an approximately planar conformation. The Fe···Fe distance between the two ferrocenyl units is 6.761 (10), 9.043 (7), and 9.172 (6) Å for the compounds **1**, **2** and **3**, respectively. In our previous report, the four *gem*-DEE bridged diferrocenyl compounds show very similar Fe···Fe distance of 6.74–7.18 Å [40]. For the present diferrocenyl compounds, the obviously increased Fe···Fe distances of **2** and **3** could be attributed to the different orientation of the two ferrocenyl groups in crystal structures. This is probably due to the intermolecular interactions including the C–H···**π** hydrogen bonds and π···π stacking interactions. As can be seen from Fig. S6 and Table S2–4, the compounds **2** and **3** exhibit stronger C–H···**π** interactions compared to that for compound **1**. Moreover, the π···π interactions were observed for compounds **2** and **3**, while it is absent in compound **1**.

The electrochemistry of these *gem*-DEE bridged diferrocenyl compounds were investigated by cyclic voltammetry (CV) and differential pulse voltammetry (DPV) measurements. The weakly coordinating supporting electrolyte $Na[B\{C_6H_3(3,5\text{-}CF_3)_2\}_4]$ was used in electrochemical experiments. Due to the substantially suppressed ion-pairing effect, this kind of electrolyte has been proved to be very efficient to improve the resolution between the coupled oxidation processes in mixed-valence poly-ferrocene compounds [41–46]. The cyclic voltammograms and differential pulse voltammograms of these compounds are characterized by a pair of overlapping but partially resolved redox couples, indicating the stepwise one-electron oxidation of two Fc units (Fig. 3). As estimated from the DPV curves, the potential difference (ΔE) for the pairwise redox couples is 168, 156, and 152 mV for compounds **1**, **2**, and **3**, respectively (Table 2). This result suggests the moderate electronic coupling between two Fc centers over the cross-conjugated *gem*-DEE bridge [33, 36, 40]. It is noteworthy that, although the Fe···Fe distances reach up to ~9.1 Å for compounds **2** and **3**, they still exhibit comparable degree of electronic coupling in comparison to compound **1** with Fe···Fe distance of ~6.7 Å. This implies that the electronic coupling between the two Fc termini more likely occurs via the through-bond mechanism. Moreover, in the recent report by

Low and co-workers, the tris(ferrocenyl) compound FcCH=C(C≡CFc)$_2$ exhibit more strong electronic coupling (ΔE = 216 mV) over the *gem*-DEE bridge with the Fe···Fe distance up to ~10.3 Å [33]. These results are suggestive of the capability of cross-conjugated *gem*-DEE bridging ligand in mediating electronic coupling between Fc termini. The similar ΔE values also indicate that the heterocyclic pendent substituents in compounds **2** and **3** have little effects on Fc–Fc electronic coupling in the cross-conjugated system.

Fig. 4a shows UV-vis-NIR spectra recorded during the stepwise chemical oxidation of compound **1** by NOBF$_4$ [51–53]. The weak and broad low-energy absorption band around 750 nm was gradually generated in the spectrum, which is indicative of the intervalence charge transfer (IVCT) transition of the mixed-valence monocation **1**$^+$. The generation of IVCT transition was also observed with the broad absorption band at ~800 nm for **2**$^+$ and **3**$^+$, respectively (Fig. S7a and S8a). The deconvolution analysis shows that the NIR band of the mixed-valence species is composed of Gaussian-shaped sub-bands corresponding to the IVCT transition and the possible ligand-to-Fe^{III} charge transfer (LMCT) transition (Fig. 4b, Fig. S7b, and Fig. S8b). The spectroscopic parameters for IVCT band are listed in Table 3. According to the Hush model, the electronic coupling metric element (H_{ab}) can be estimated from the IVCT band parameters by using the equation: $H_{ab} = 2.05 \times 10^{-2}[(\nu_{max}\, \varepsilon_{max}\, \Delta\nu_{1/2})^{1/2}/r_{ab}]$ [48]. The value of H_{ab} is calculated to be 560, 470, and 382 cm^{-1} for compounds **1**, **2**, and **3**, respectively (Table 3). These results suggest that the monocation for these *gem*-DEE-bridged diferrocenyl compounds can be described as the weakly coupled Robin–Day class II mixed-valence species [55].

The electronic structure of these diferrocenyl compounds was studied by DFT calculations at the B3LYP level of theory with 6-31G** basis set. As shown in Fig. 5, the HOMO on the *gem*-DEE backbone is the out-of-phase combination of three π orbitals on two acetylene and one ethene units, and it is the in-phase combination of the three π* orbitals for LUMO. This result is indicative of π electron delocalization across the *gem*-DEE bridge, as that revealed by the theoretical investigations on free *gem*-DEE ligand by Ren and co-workers [39]. The HOMO of these diferrocenyl compounds has dominant contribution from the Fc termini mainly on the Fe 3d orbitals, while the electron density on Fc units is significantly reduced in the LUMO. The pendent substituents in these compounds have little contribution to the frontier orbitals due to their saturated structure. DFT calculations on the monocation $\mathbf{1}^+$ show the predominant spin localization on one Fc unit along with some contribution from half of the *gem*-DEE skeleton (Fig. 6). This result suggests the localized oxidation on Fc unit in the monocation $\mathbf{1}^+$ that is characteristic for the electronic structure of class II mixed-valence species [56–58].

4. Conclusions

In this study, a series of diferrocenyl compounds bridged by cross-conjugated *gem*-DEE ligands with different pendent substituents including cyclohexane, tetrahydro-2*H*-pyran, and tetrahydro-2*H*-thiopyran were synthesized and characterized. The X-ray crystallographic study reveals the varying Fe···Fe distances between the Fc termini in the crystal structures of these compounds, which reaches up to ~9 Å for compounds **2** and **3**. The *gem*-DEE-bridged Fc termini exhibit moderate electronic coupling in this cross-conjugated system. The electronic coupling only show slight attenuation with increasing Fe···Fe distances from **1** to **3**.

Hush analysis on IVCT bands of the monocation species is suggestive of the Robin–Day class II mixed-valence system.

Acknowledgements

We acknowledge support by the National Natural Science Foundation of China (No. 21002082) and the Nanhu Scholars Program for Young Scholars of XYNU.

Appendix A. Supplementary material

Crystal data and structure refinements summary for compounds **1**–**3**; Analysis of C–H$\cdots\pi$ (Cp-ring) interactions for compound **1**–**3**; ^{1}H and ^{13}C NMR spectra of **1**, **2a**, **2**, **3a**, **3**; UV-Vis-NIR spectra recorded during stepwise chemical oxidation of compound **2** and **3** by $NOBF_4$ in CH_2Cl_2; The Gaussian deconvolution of NIR absorptions for the monocation **2**$^+$ and **3**$^+$.

References

[1] P.J. Low, Coord. Chem. Rev. 257 (2013) 1507.

[2] J.-F. Halet, C. Lapinte, Coord. Chem. Rev. 257 (2013) 1584.

[3] W.-Y. Wong, C.-L. Ho, Coord. Chem. Rev. 250 (2006) 2627.

[4] W.-Y. Wong, Comments Inorg. Chem. 26 (2005) 39.

[5] P. Aguirre-Etcheverry, D. O'Hare, Chem. Rev. 110 (2010) 4839.

[6] D.M. D'Alessandro, F.R. Keene, Chem. Rev. 106 (2006) 2270.

[7] K.D. Demadis, C.M. Hartshorn, T.J. Meyer, Chem. Rev. 101 (2001) 2655.

[8] R.F. Winter, Organometallics 33 (2014) 4517.

[9] A. Hildebrandt, H. Lang, Organometallics 32 (2013) 5640.

[10] R. Breuer, M. Schmittel, Organometallics 32 (2013) 5980.

[11] R. Breuer, M. Schmittel, Organometallics 31 (2012) 6642.

[12] R. Breuer, M. Schmittel, Organometallics 31 (2012) 1870.

[13] W.-Y. Wong, G.-L. Lu, K.-F. Ng, K.-H. Choi, Z. Lin, J. Chem. Soc. Dalton Trans. 22 (2001) 3250.

[14] W.-Y. Wong, G.-L. Lu, K.-F. Ng, C.-K. Wong, K.-H. Choi, J. Organomet. Chem. 637–639 (2001) 159.

[15] W.-Y. Wong, K.-Y. Ho, S.-L. Ho, Z. Lin, J. Organomet. Chem. 683 (2003) 341.

[16] W.-Y. Wong, G.-L. Lu, K.-H. Choi, Y.-H. Guo, J. Organomet. Chem. 690 (2005) 177.

[17] S. Mishra, S. Dewangan, S. Giri, S. M. Mobin, S. Chatterjee, Eur. J. Inorg. Chem. 35 (2016) 5485.

[18] S. Roué, H. Sahnoune, L. Toupet, J.-F. Halet, C. Lapinte, Organometallics 35 (2016) 2057.

[19] A.K. Diallo, J.-C. Daran, F. Varret, J. Ruiz, D. Astruc, Angew. Chem. Int. Ed. 48 (2009) 3141.

[20] W.Y. Chan, A.J. Lough, I. Manners, Angew. Chem. Int. Ed. 46 (2007) 9069.

[21] R.C. Quardokus, Y. Lu, N.A. Wasio, C.S. Lent, F. Justaud, C. Lapinte, S.A. Kandel, J. Am. Chem. Soc. 134 (2012) 1710.

[22] S.W. Lehrich, A. Hildebrandt, M. Korb, H. Lang, J. Organomet. Chem. 847 (2017) 105.

[23] G.-T. Xu, B. Li, J.-Y. Wang, D.-B. Zhang, Z.-N. Chen, Chem. Eur. J. 21 (2015) 3318.

[24] Y.-P. Ou, J. Zhang, M.-X. Zhang, F. Zhang, D. Kuang, F. Hartl, S. H. Liu, Inorg. Chem. 56 (2017) 11074.

[25] S. Muratsugu, M. Kishida, R. Sakamoto, H. Nishihara, Chem. Eur. J. 19 (2013) 17314.

[26] A. Sundararaman, K. Venkatasubbaiah, M. Victor, L. N. Zakharov, A. L. Rheingold, F. Jäkle, J. Am. Chem. Soc. 128 (2006) 16554.

[27] J.-P. Launay, Chem. Soc. Rev. 30 (2001) 386.

[28] Z. Cao, B. Xi, D.S. Jodoin, L. Zhang, S.P. Cummings, Y. Gao, S.F. Tyler, P.E. Fanwick, R.J. Crutchley, T. Ren, J. Am. Chem. Soc. 136 (2014) 12174.

[29] G.-L. Xu, R.J. Crutchley, M.C. DeRosa, Q.-J. Pan, H.-X. Zhang, X. Wang, T. Ren, J. Am. Chem. Soc. 127 (2005) 13354.

[30] G.-L. Xu, G. Zou, Y.-H. Ni, M.C. DeRosa, R.J. Crutchley, T. Ren, J. Am. Chem. Soc. 125 (2003) 10057.

[31] K.B. Vincent, Q. Zeng, M. Parthey, D.S. Yufit, J.A.K. Howard, F. Hartl, M. Kaupp, P.J. Low, Organometallics 32 (2013) 6022.

[32] M.I. Bruce, A. Burgun, M.A. Fox, M. Jevric, P.J. Low, B.K. Nicholson, C.R. Parker, B.W. Skelton, A.H. White, N.N. Zaitseva, Organometallics 32 (2013) 3286.

[33] K.B. Vincent, J.B.G. Gluyas, Q. Zeng, D.S. Yufit, J.A.K. Howard, F. Hartl, P.J. Low, Dalton Trans. 46 (2017) 5522.

[34] K.B. Vincent, J.B.G. Gluyas, S. Gückel, Q. Zeng, F. Hartl, M. Kaupp, P.J. Low, J. Organomet. Chem. 821 (2016) 40.

[35] G.-L. Xu, B. Xi, J.B. Updegraff, J.D. Protasiewicz, T. Ren, Organometallics 25 (2006) 5213.

[36] W.P. Forrest, M.M.R. Choudhuri, S.M. Kilyanek, S.N. Natoli, B.M. Prentice, P.E. Fanwick, R.J. Crutchley, T. Ren, Inorg. Chem. 54 (2015) 7645.

[37] W.P. Forrest, Z. Cao, K.M. Hassell, B.M. Prentice, P.E. Fanwick, T. Ren, Inorg. Chem. 51 (2012) 3261.

[38] S.N. Natoli, T.J. Azbell, P.E. Fanwick, M. Zeller, T. Ren, Organometallics 35 (2016) 3594.

[39] Z. Cao, T. Ren, Organometallics 30 (2011) 245.

[40] Y. Fan, H.-M. Li, G.-D. Zou, X. Zhang, Y.-L. Pan, K.-K. Cao, M.-L. Zhang, P.-L. Ma, H.-T. Lu, Organometallics 36 (2017) 4278.

[41] M. Rosenblum, N. Brawn, J. Papenmeier, M. Applebaum, J. Organometallic Chem. 6 (1966) 173.

[42] P.J. Kropp, S.A. McNeely, R.D. Davis, J. Am. Chem. Soc. 105 (1983) 6907.

[43] D.L. Reger, T.D. Wright, C.A. Little, J.J.S. Lamba, M.D. Smith, Inorg. Chem. 40 (2001) 3810.

[44] G.M. Sheldrick, Acta Cryst. C71 (2015) 3.

[45] W.E. Geiger, F. Barrière, Acc. Chem. Res. 43 (2010) 1030.

[46] M.S. Inkpen, S. Scheerer, M. Linseis, A.J.P. White, R.F. Winter, T. Albrecht, N.J. Long, Nat. Chem. 8 (2016) 825.

[47] A.K. Diallo, C. Absalon, J. Ruiz, D. Astruc, J. Am. Chem. Soc. 133 (2011) 629.

[48] Y. Li, M. Josowicz, L.M. Tolbert, J. Am. Chem. Soc. 132 (2010) 10374.

[49] S.W. Lehrich, A. Hildebrandt, M. Korb, H. Lang, J. Organomet. Chem. 792 (2015) 37.

[50] E.A. Poppitz, A. Hildebrandt, M. Korb, H. Lang, J. Organomet. Chem. 752 (2014) 133.

[51] A. Vecchi, N.R. Erickson, J.R. Sabin, B. Floris, V. Conte, M. Venanzi, P. Galloni, V.N. Nemykin, Chem. Eur. J. 21 (2015) 269.

[52] V.N. Nemykin, A.A. Purchel, A.D. Spaeth, M.V. Barybin, Inorg. Chem. 52 (2013) 11004.

[53] L.E. Wilson, C. Hassenrück, R.F. Winter, A.J.P. White, T. Albrecht, N.J. Long, Angew. Chem. Int. Ed. 56 (2017) 6838.

[54] N.S. Hush, Coord. Chem. Rev. 64 (1985) 135.

[55] M.B. Robin, P. Day, Adv. Inorg. Chem. Radiochem. 9 (1967) 247.

[56] M. Parthey, M. Kaupp, Chem. Soc. Rev. 43 (2014) 5067.

[57] N.J. Brown, H.N. Lancashire, M.A. Fox, D. Collison, R. Edge, D.S. Yufit, J.A.K. Howard, M.W. Whiteley, P.J. Low, Organometallics 30 (2011) 884.

[58] O. Gidron, Y. Diskin-Posner, M. Bendikov, Chem. Eur. J. 19 (2013) 13140.

Scheme 1. Synthetic route for compounds **1–3**.

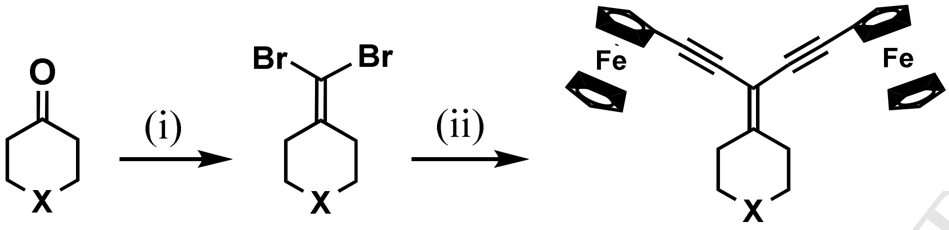

X = C (**1**), O (**2**), S (**3**).

Conditions: (i) CBr_4 (2.0 equiv), PPh_3 (4.0 equiv), heptane, reflux 48 h; (ii) FcC≡CH (3.0 equiv), $Pd(PPh_3)_2$ (0.13 equiv), CuI (0.33 equiv), Et_3N, 95 ^{o}C, 24 h.

Table 1. Selected bond lengths (Å) and angles (deg) for compounds **1–3**.

	1	**2**	**3**
C21–C22	1.179(4)	1.180(4)	1.193(4)
C24–C25	1.198(4)	1.195(4)	1.190(4)
C23–C26	1.347(4)	1.348(5)	1.340(4)
Fe1···Fe2	6.761(10)	9.043(7)	9.172(6)
C22–C23–C24	113.5(3)	115.6(3)	115.3(3)

Table 2. Electrochemical fata from DPV measurements (vs Ag/AgCl).

Compd	Ox_1, mV	Ox_2, mV	ΔE, mV	K_c
1	40	208	168	692
2	68	224	156	434
3	56	208	152	371

Table 3. Parameters for the IVCT band of **1**$^+$–**3**$^+$.

Compd	ν_{max} (cm^{-1})	ε (L mol^{-1} cm^{-1})	$\Delta\nu_{1/2}$ (cm^{-1})	r_{ab} (Å)	$\Delta\nu_{1/2}$(theor) (cm^{-1})	H_{ab} (cm^{-1})
1$^+$	14278	426	5557	6.761	5743	560
2$^+$	12950	901	3650	9.043	5469	470
3$^+$	12300	712	3300	9.172	5330	382

Fig. 1. The *gem*-DEE bridged diferrocenyl compounds **1**–**3**.

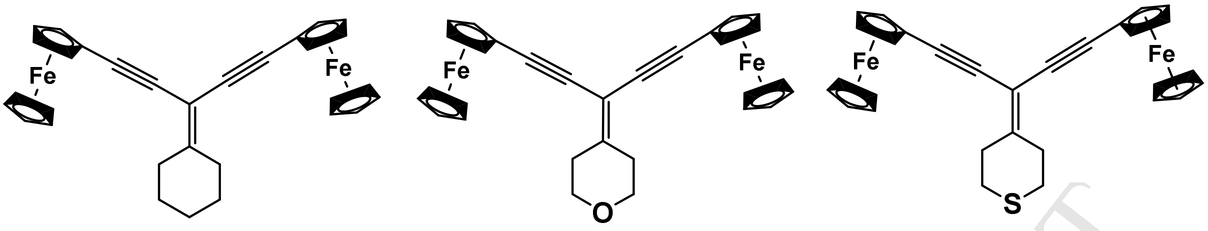

1 **2** **3**

Fig. 2. X-ray crystal structures of compounds **1**–**3**. The ellipsoids are drawn at the 30% probability level. H atoms are omitted for clarity.

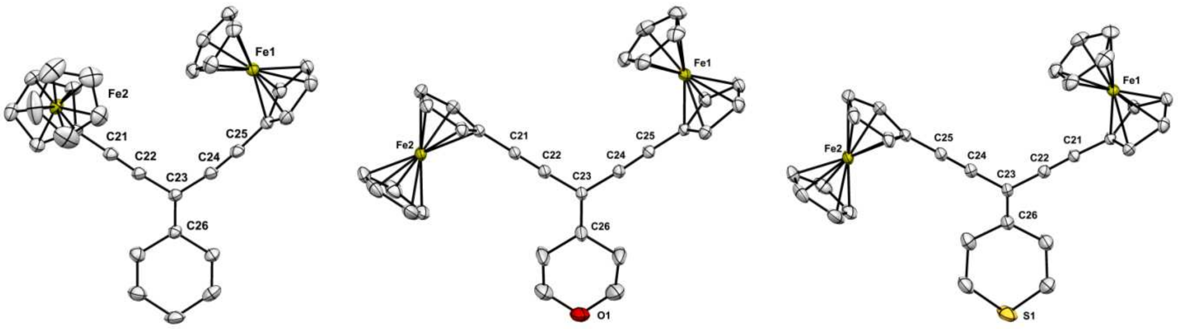

1 **2** **3**

Fig. 3. CV (top) and DPV (bottom) of compounds **1** (a), **2** (b), and **3** (c) recorded in CH_2Cl_2 solution containing 0.01 M $Na[B\{C_6H_3(3,5\text{-}CF_3)_2\}_4]$ at room temperature. Scan rate: 50 mV s^{-1}.

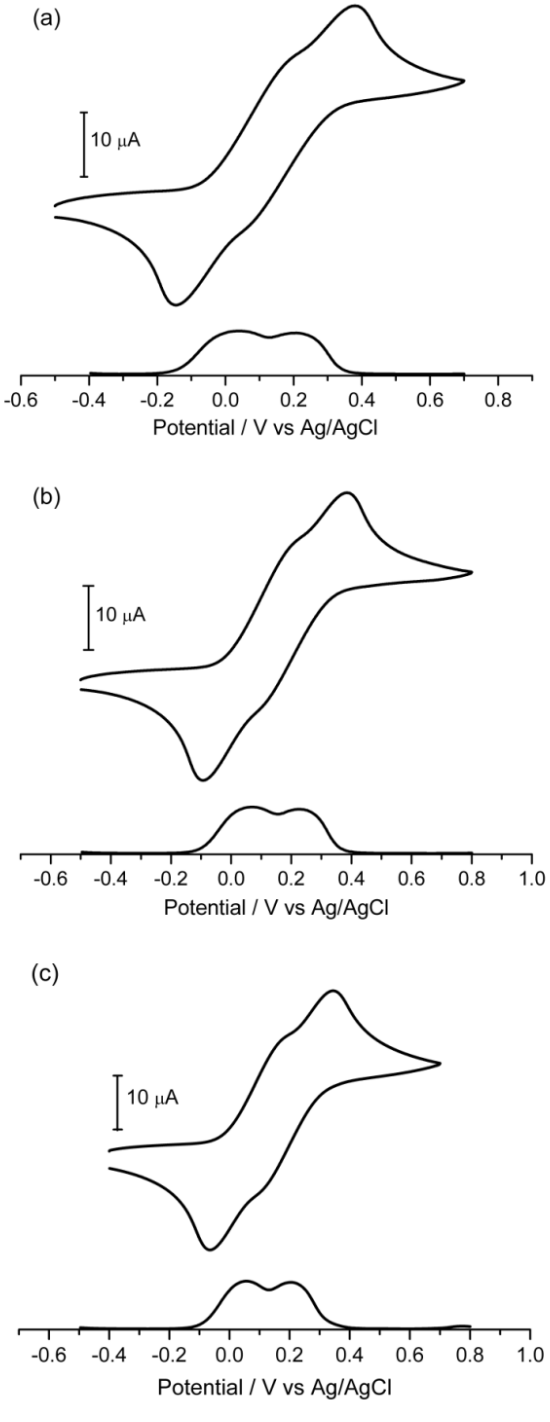

Fig. 4. (a) UV-Vis-NIR spectra recorded during stepwise chemical oxidation of compound **1** by $NOBF_4$ in CH_2Cl_2. (b) The Gaussian deconvolution of NIR absorptions for the monocation $\mathbf{1}^+$.

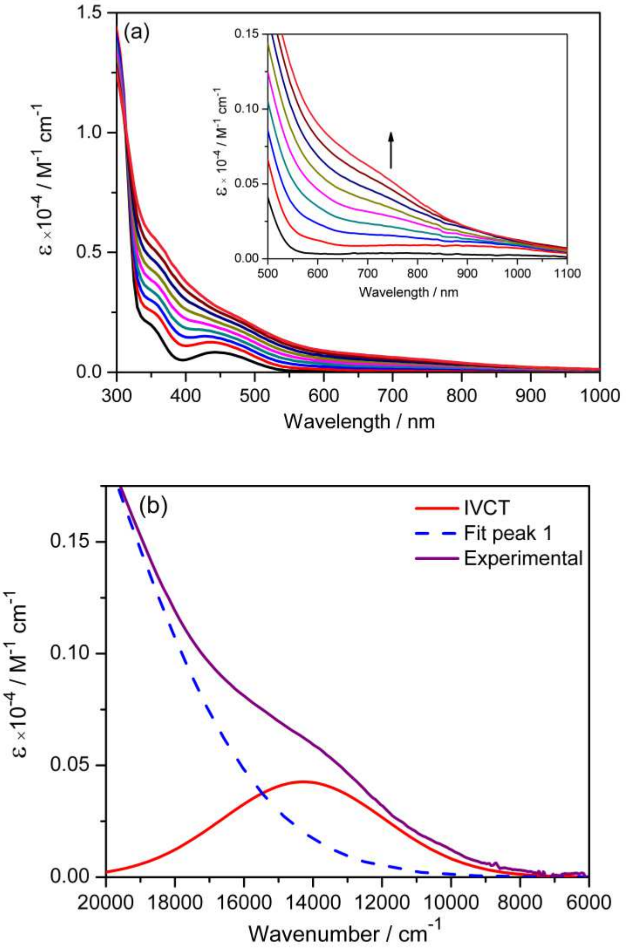

Fig. 5. HOMO and LUMO for compounds **1–3**.

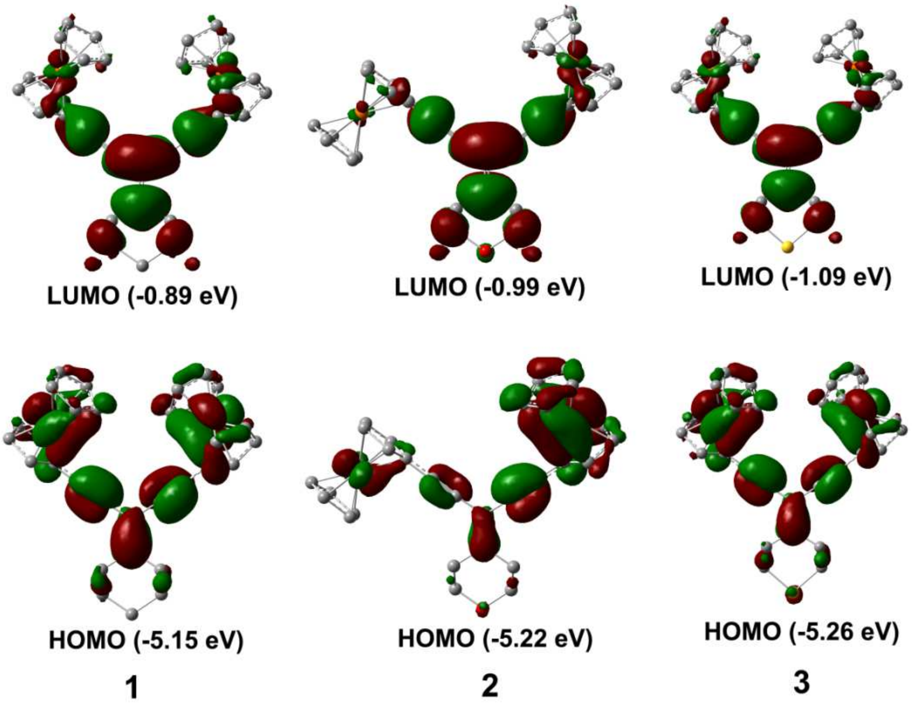

Fig. 6. Spin-density isosurface plot (left) and SOMO (right) of the monocation $\mathbf{1}^+$.

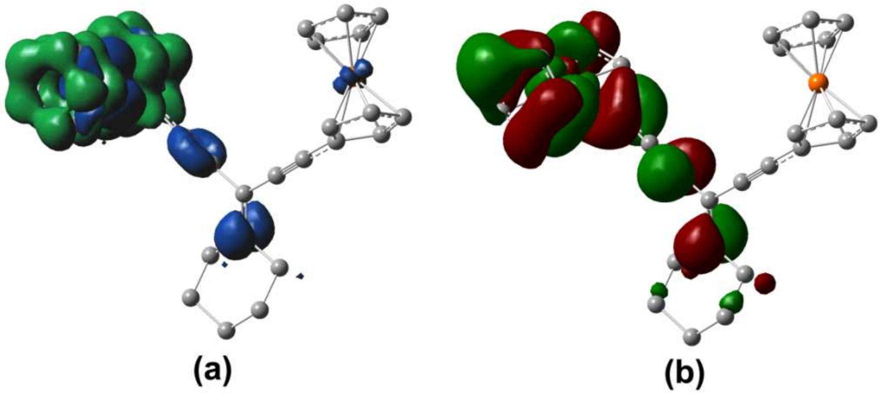

Highlights

- A series of *gem*-DEE bridged diferrocenyl compounds were synthesized.

- The Fe···Fe distance between the two ferrocenyl termini reaches up to ~9 Å.

- The cross-conjugated systems exhibit moderate electronic coupling between two ferrocenyl termini.